

Instabilities of Current-Carrying Relativistic Jets

Andrea Mignone ^{1, @}

¹ : Dipartimento di Fisica, Università di Torino

I discuss some recent results on the linear and nonlinear stability analysis of Newtonian and relativistic magnetized jets carrying helical magnetic fields.

Nonlinear evolution is investigated with the aid of three-dimensional numerical simulations using the PLUTO code. The role of Kelvin-Helmholtz, current- and pressure-driven instabilities and their impact on the jet morphology, jet braking and overall stability is analyzed.

Subject : : oral
Topics : : Astrophysics

Instabilities of Current-Carrying Relativistic and Newtonian Jets

Andrea Mignone¹

**Collaborators: G. Bodo², P. Rossi², G. Mamatshvili³,
M. Anjiri¹, A. Ferrari¹**

¹Dipartimento di Fisica Generale, Turin University, Torino (TO), Italy

²INAF Osservatorio Astronomico di Torino, Pino Torinese (TO), Italy

³Department of Physics, Tbilisi State University, Georgia

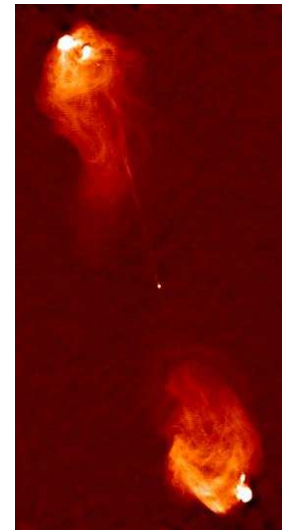
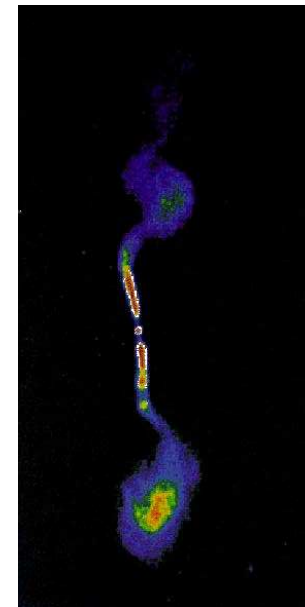
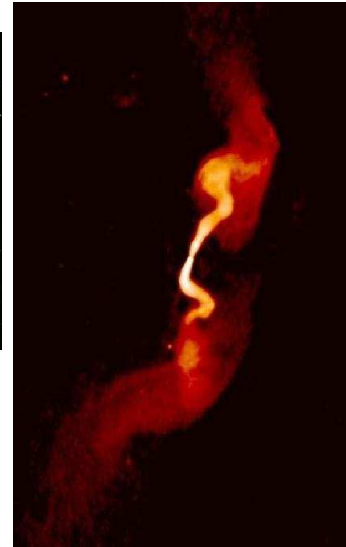
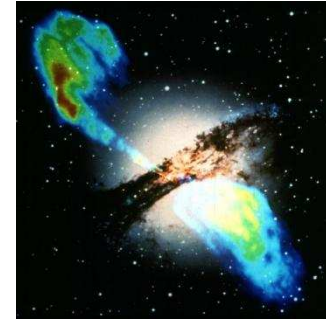


Outline

- Scientific background:
 - Morphology of extragalactic jets;
 - 3D numerical simulations of current-carrying relativistic jets;
- Fluid instabilities in non-rotating jets
- Linear stability analysis of cold relativistic MHD jets
- Nonlinear evolution: numerical simulations
- Conclusions

Astrophysical Background

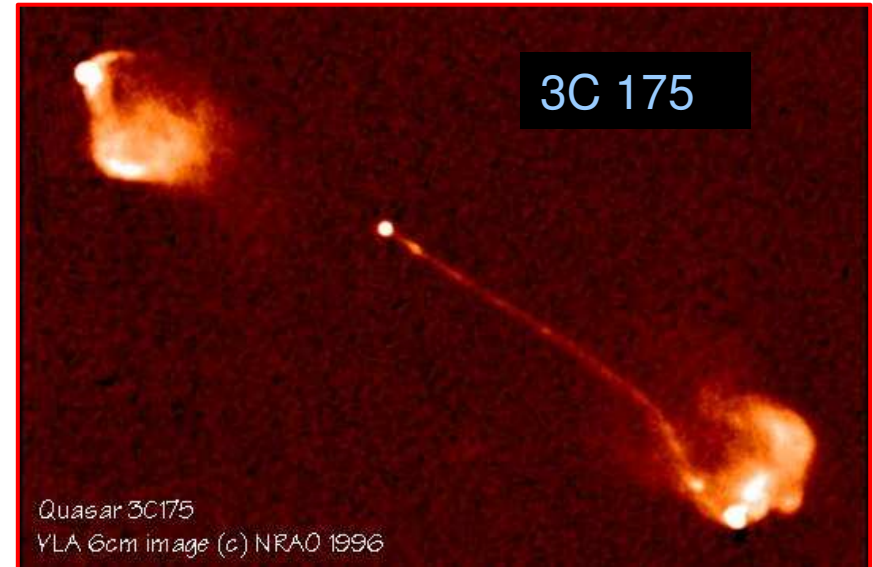
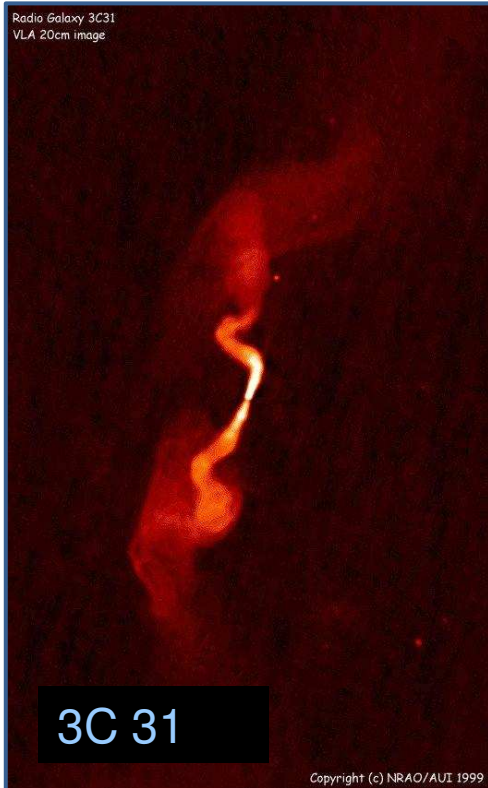
- Observations of AGN jet show change in propagation direction (see Kovalev talk) and morphology;
- Bending and deflection can be induced by different physical mechanisms → instabilities / interaction with the ambient;
- Jet curvature may enhance energy and momentum dissipation leading to substantial deceleration;
- Understanding the basic physical mechanisms crucial to address many unanswered questions.



AGN Jets: FRI / FRII Dicothomy

- FR I: Low power sources dominated by jet emission, two-sided jets, typically found in rich clusters.

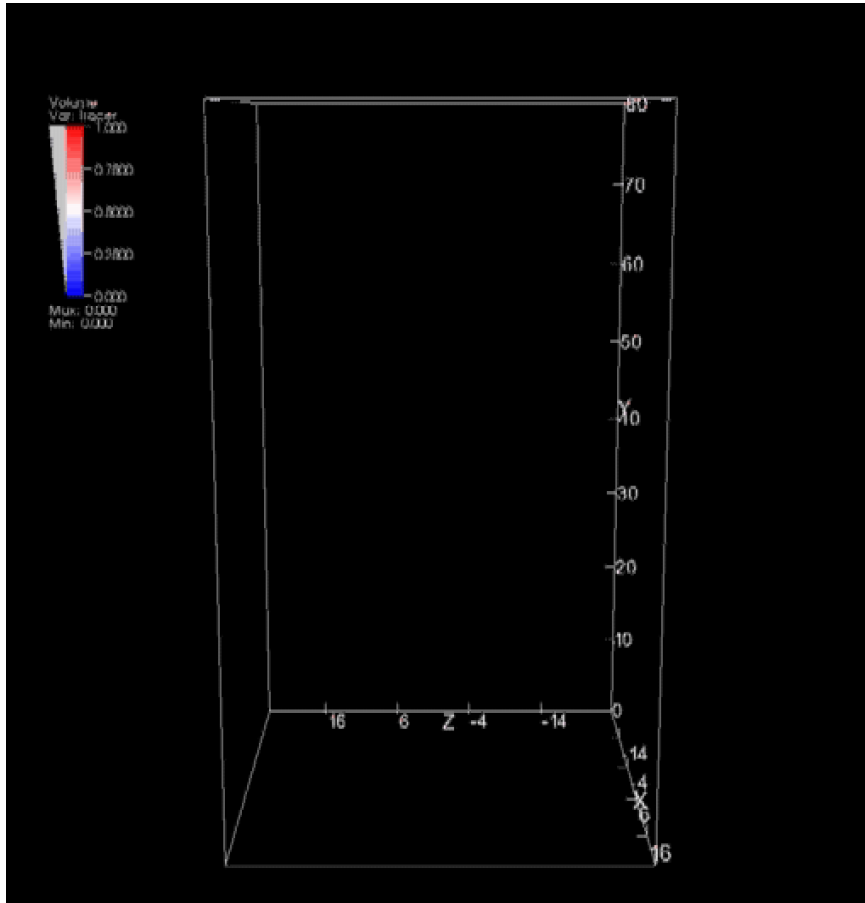
- FR II: High power sources, one-sided jet dominated by lobe emission, found isolated or in poor groups.



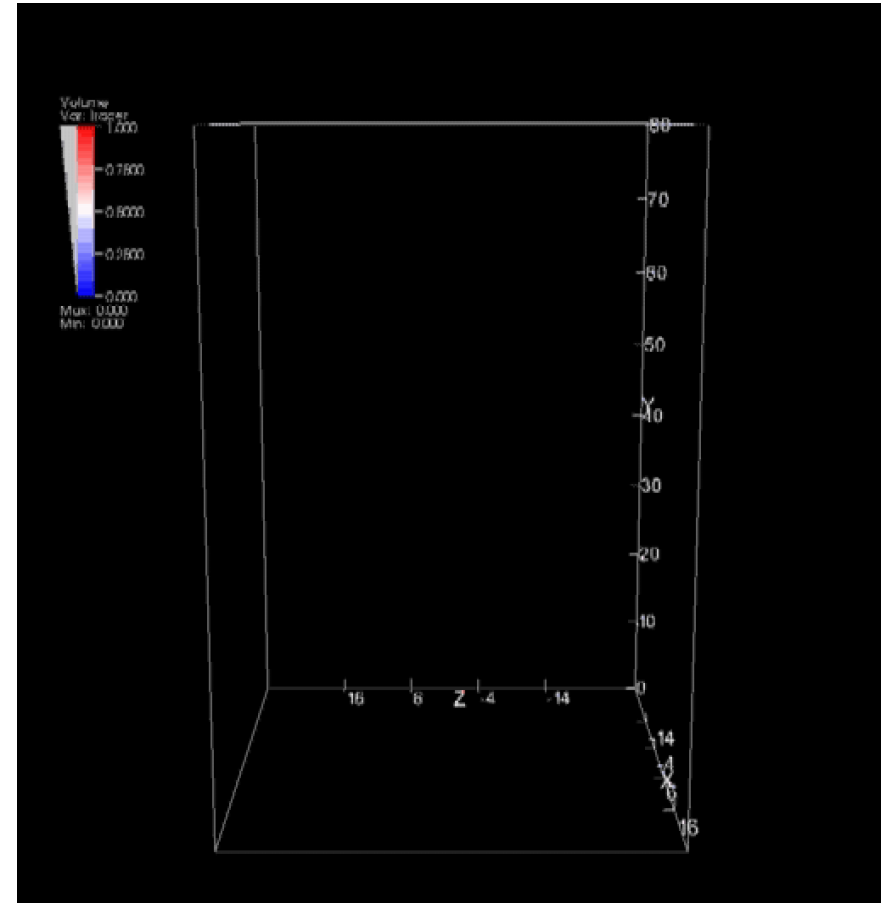
AGN Jets: 3D Simulations

- Relativistic MHD (RMHD) 3D simulations of AGN jets¹:

$\gamma = 10$, poloidal magnetic field (B_z);



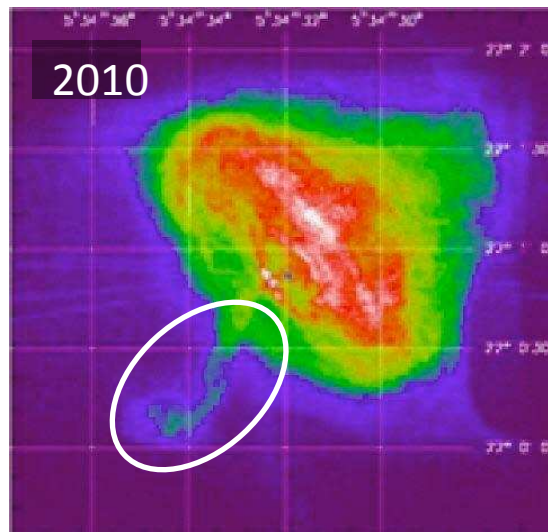
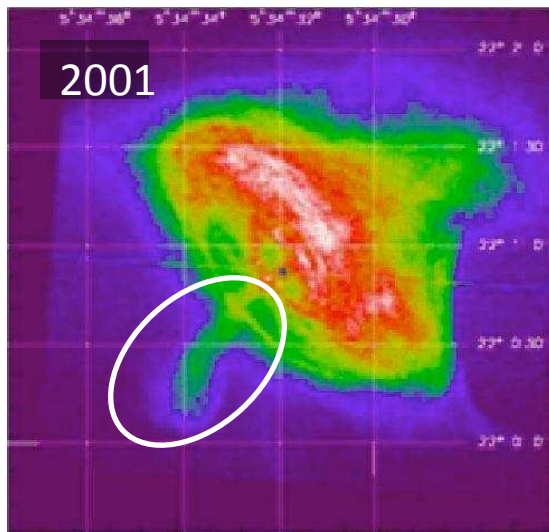
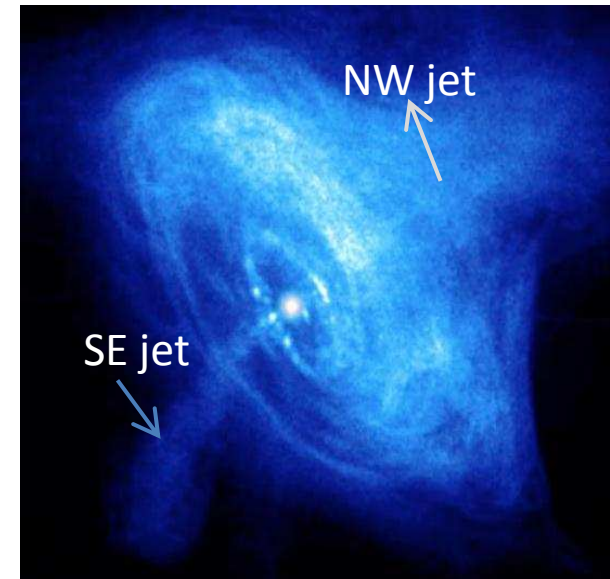
$\gamma = 10$, toroidal magnetic field (B_ϕ);



¹Mignone et al, MNRAS (2010) 402, 7

Jet from the Crab Nebula

- Jet from the interaction between pulsar wind and collimating action of azimuthal B (hoop stress) ^{1,2}.
- In the SE jet material flows with $v/c \sim 0.4$ slowing down to ~ 0.02 into the nebula;
- SE jet morphology is “S” shaped and show remarkable time variability:



¹Komissarov & Lyubarski 2003,2004; ²Del Zanna et al. 2004

Crab Jet: 3D Simulations

- Relativistic MHD (RMHD) jets from the Crab Nebula¹

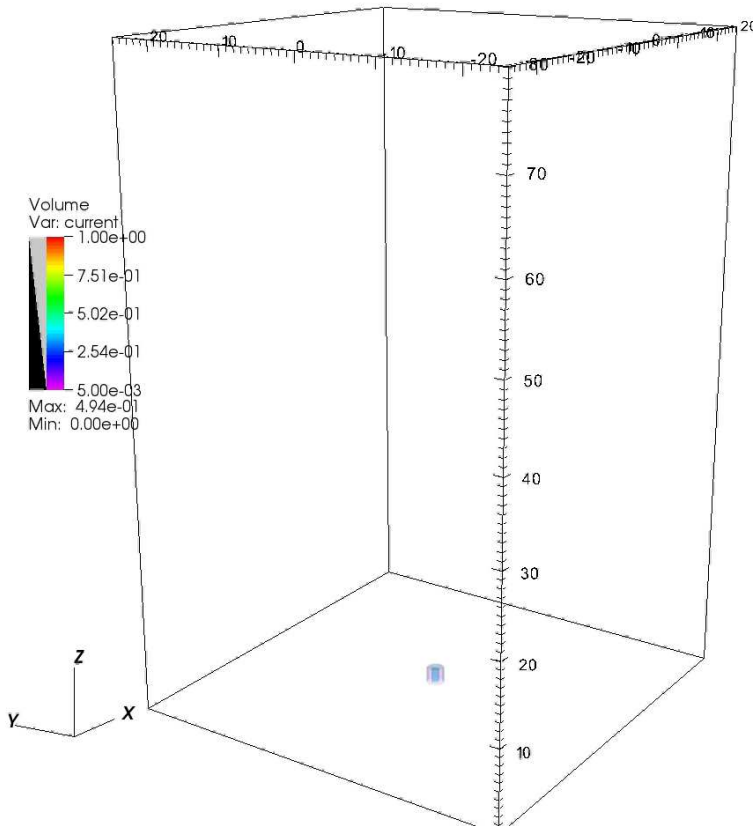
$$\gamma = 2, \beta \approx 0.6$$

$$\gamma = 4, \beta \approx 1.2$$

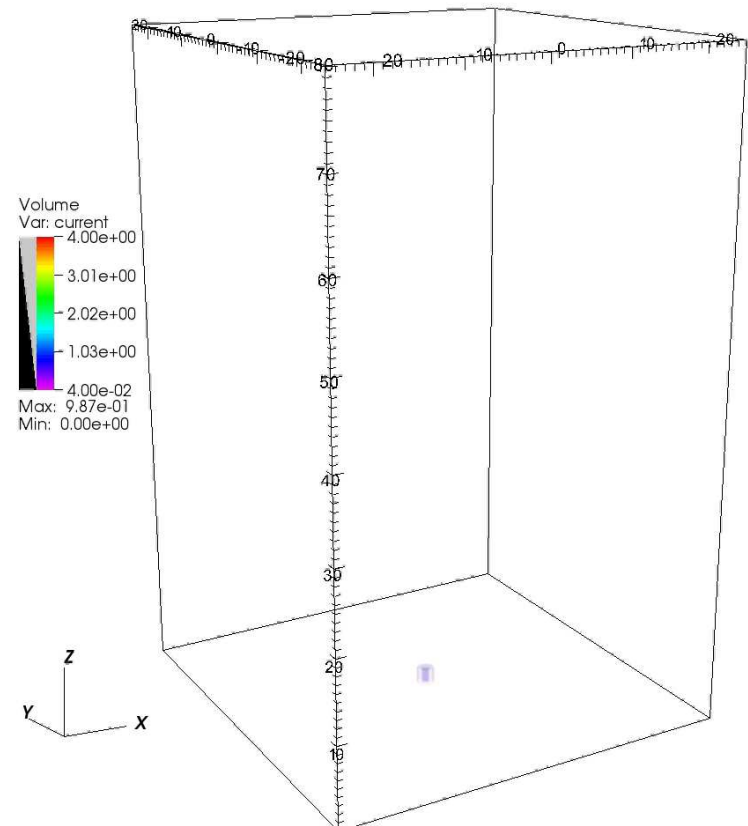
www.videomach.com

www.videomach.com

Case A2, $t=0.00$ (yrs)

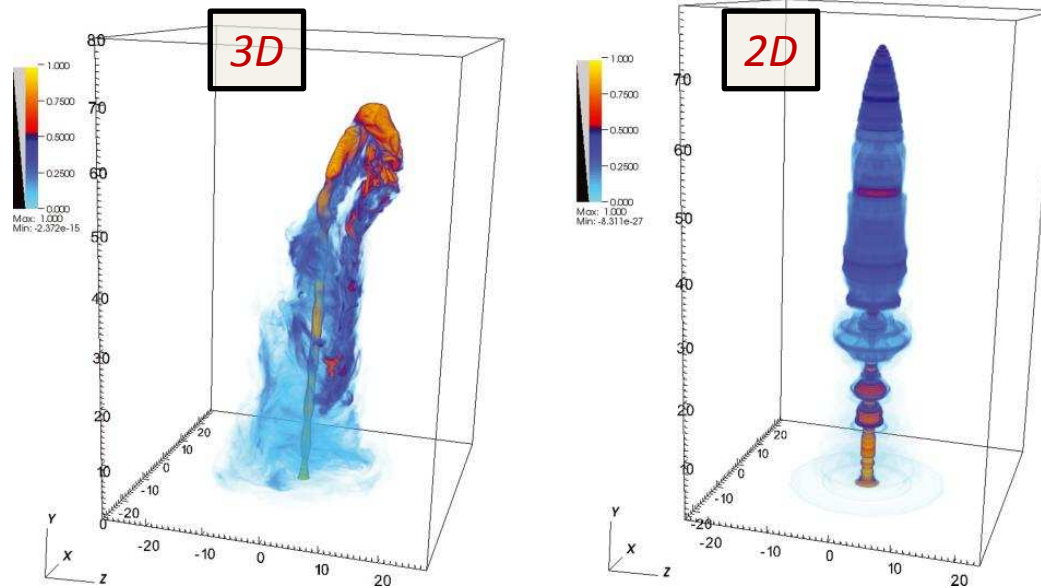


Case B2, $t=0.00$ (yrs)



¹Mignone et al, MNRAS (2013) 436, 1102

General features of 3D models

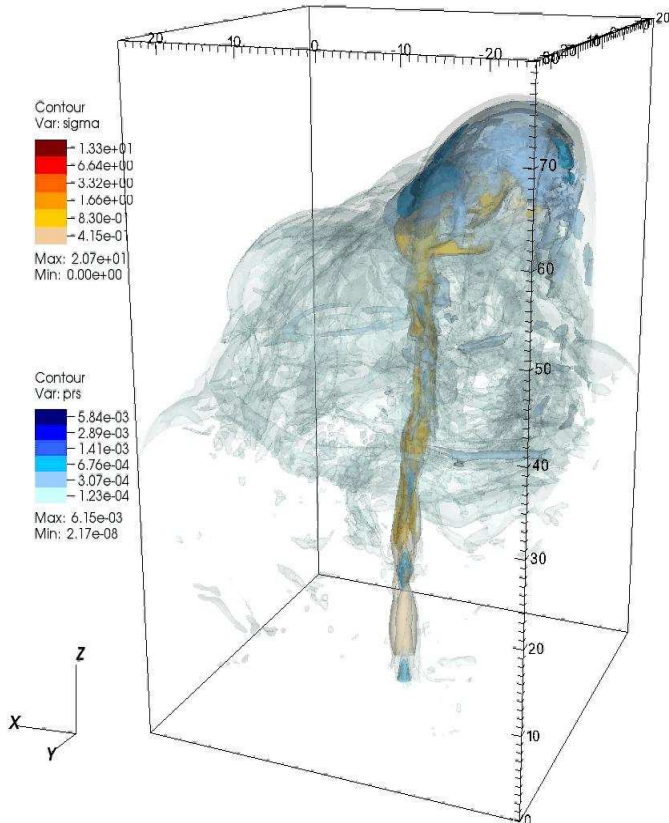


- 3D models very different from 2D axisymmetric models;
- The presence of a toroidal field de-stabilizes the structure:
 - non-axisymmetric deformation
 - time-dependent deflections;
- Deflection time scale (crab) \approx 5-10 years (compatible with observations)

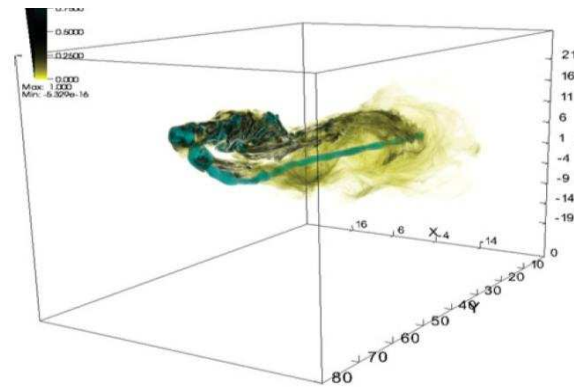
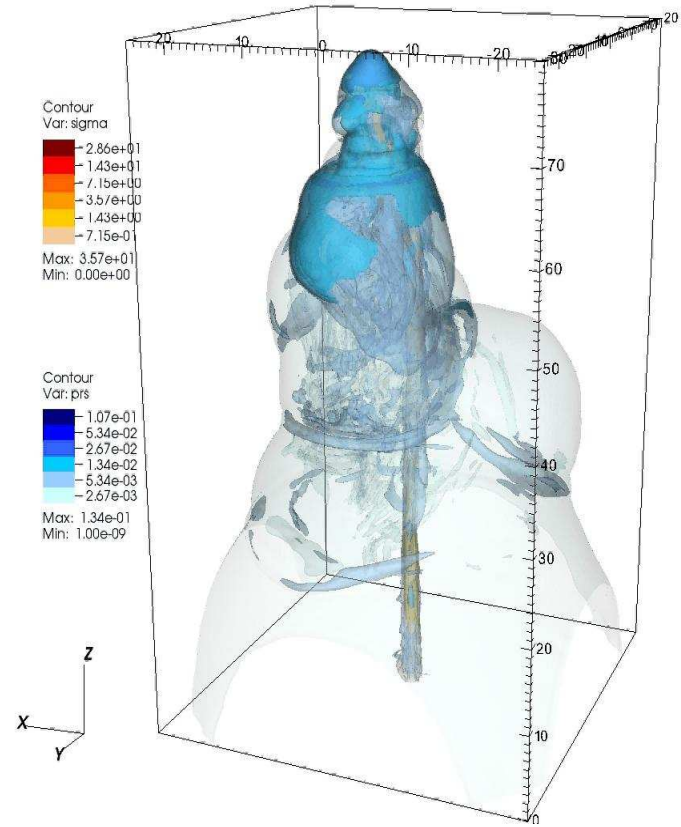
Which instabilities are (precisely) at work ?

www.videomach.com

Case A2, t=130.09 (yrs)



Case B2, t=47.60 (yrs)



Let's take one step back...

Instabilities in non-rotating jets

- Non-rotating jets may be prone to three types of instabilities,

Kelvin-Helmholtz (KHI):

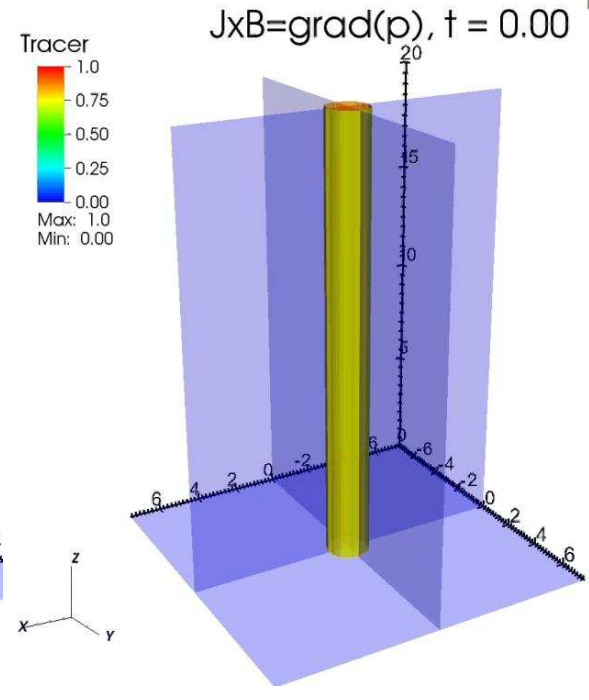
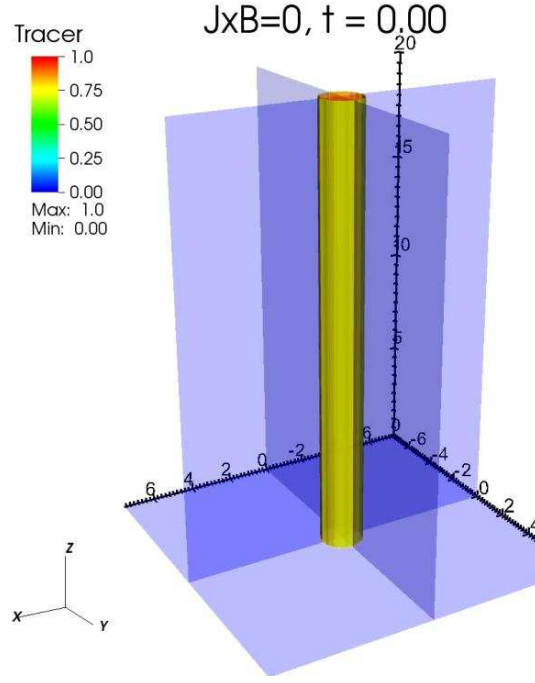
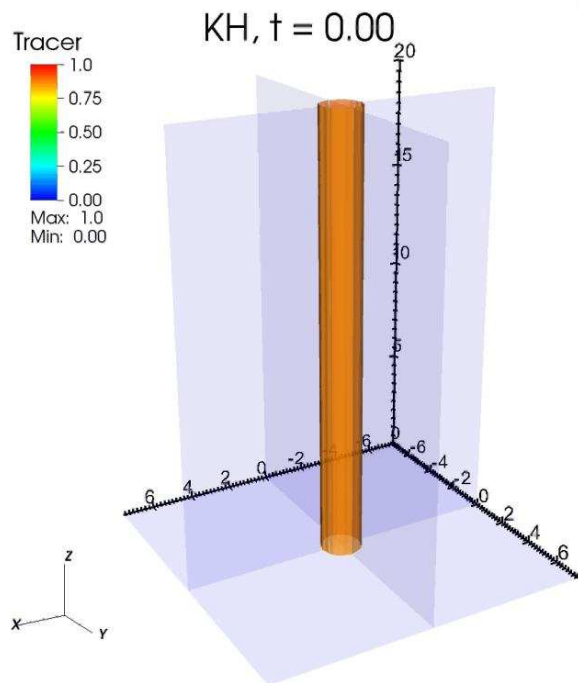
driven by relative velocity shear \rightarrow mixing, mom & energy transfer, entrainment .

Current-Driven (CDI) :

driven by \parallel component of current, small pitch \rightarrow helical deformation.

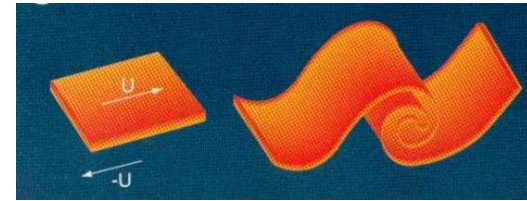
Pressure-Driven (PDI):

driven by the \perp component of current \rightarrow interchange modes (like RT)

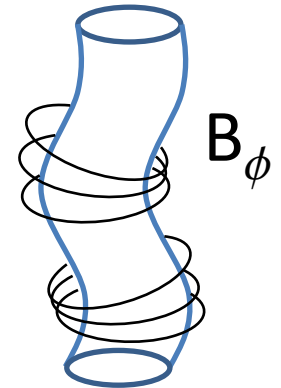


Principles of Instabilities

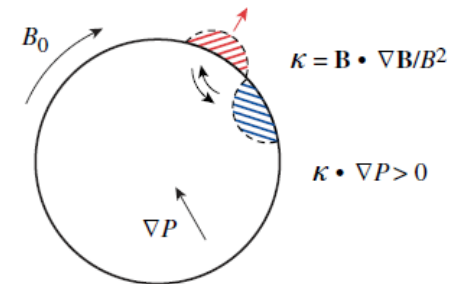
- KHI: perturbation induces large pressure in concavities so the amplitude of the oscillation grows up
→ rolling up of the interface



- CDI: perturbation brings field lines closer on the concave side and further apart on the convex side. The larger magnetic pressure will bend the deformation even more leading to an instability. Driven when $J \parallel B$.



- PDI: unfavourable field curvature relative to the pressure gradient ($\kappa \cdot B > 0$): pressure force pushes the plasma outwards from the inside of the field line curvature. Driven when $J \perp B$.



- Fundamental features of instability can be highlighted using linearized form MHD / RMHD equations, in the limit of small perturbations.

Stability of RMHD Jets: Linear Analysis

- We consider cold relativistic MHD (RMHD) flows¹ ($p = 0$):

$$\frac{\partial}{\partial t}(\gamma\rho) + \nabla \cdot (\gamma\rho\mathbf{v}) = 0,$$

$$\gamma\rho \frac{\partial}{\partial t}(\gamma\mathbf{v}) + \gamma\rho(\mathbf{v} \cdot \nabla)(\gamma\mathbf{v}) = \mathbf{J} \times \mathbf{B} + \frac{(\nabla \cdot \mathbf{E})\mathbf{E}}{4\pi},$$

$$\frac{\partial \mathbf{B}}{\partial t} = -\nabla \times \mathbf{E}, \quad \frac{\partial \mathbf{E}}{\partial t} = \nabla \times \mathbf{B} - 4\pi\mathbf{J},$$

- In cylindrical coordinates (r, ϕ, z) assume radial equilibrium such that $r, \partial/\partial\phi = \partial/\partial z = 0$;

$$\rightarrow \begin{cases} \mathbf{v} = \kappa(r)\mathbf{B} + \Omega(r)r\mathbf{e}_\phi \\ \mathbf{E} = -\Omega r B_z \mathbf{e}_r \end{cases}$$

- The only nontrivial Eq.:

$$\left(\frac{\partial p}{\partial r} - \frac{w\gamma^2 v_\phi^2}{r} \right) \hat{r} = (\nabla \cdot \mathbf{E})\mathbf{E} + \mathbf{J} \times \mathbf{B}$$

- For cold ($p=0$), non-rotating jet \rightarrow Force free conditions

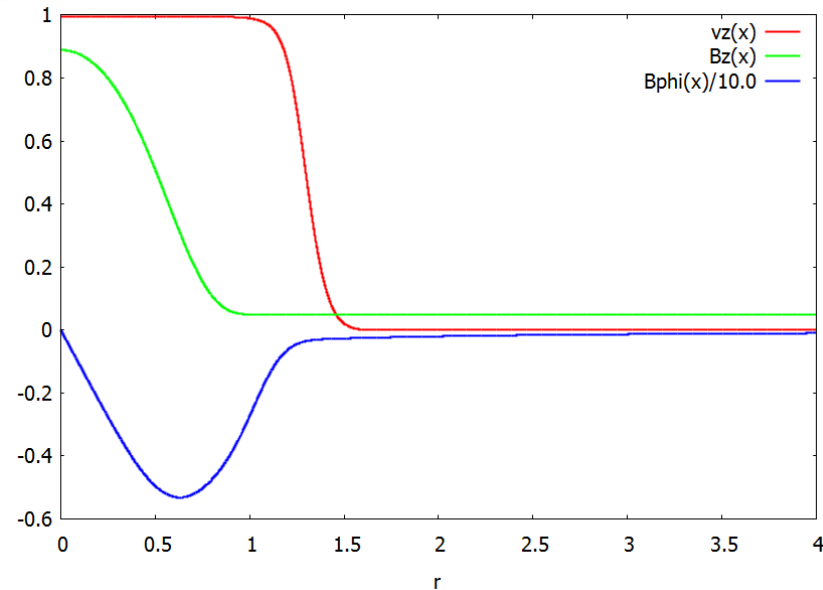
$$\rightarrow (\nabla \cdot \mathbf{E})\mathbf{E} + \mathbf{J} \times \mathbf{B} = \mathbf{0}$$

¹Bodo et al, MNRAS (2013) 434, 303

Equilibrium Model

- Equilibrium profiles

$$\left\{ \begin{array}{l} \gamma_z(r) = 1 + \frac{\gamma_c - 1}{\cosh(r/r_j)^6} \\ H^2 = B_\phi^2 - \Omega^2 r^2 B_z^2 = \frac{H_c^2}{r^2} \left[1 - \exp\left(-\frac{r^4}{a^4}\right) \right] \\ B_z^2 = B_{zc}^2 - \frac{H_c^2 \sqrt{\pi}}{(a/r_j)^2} \operatorname{erf}\left(\frac{r^2}{a^2}\right) \end{array} \right.$$



- We adopt constant density so that the model depends on 3 parameters:

- On-axis magnetic pitch:

$$P_c \equiv \left| \frac{r B_z}{B_\phi} \right|_{r=0}$$

- Lorentz factor:

$$\gamma_c = 1 / \sqrt{1 - v_c^2}$$

- Magnetization:

$$M_a^2 \equiv \frac{(\rho \gamma_c^2)}{\langle \mathbf{B}^2 \rangle}$$

Linear Stability: Equations

- Linearization proceeds by normal mode analysis.

Writing flow quantities as $Q = Q_0 + Q_1$ where $|Q_1| \ll |Q_0|$ one obtains

$$\left\{ \begin{array}{l} \dots \text{ [lots of algebra] } \dots \\ \rho_0 \gamma_0 \left(\frac{\partial}{\partial t} + \mathbf{v}_0 \cdot \nabla \right) (\gamma_1 \mathbf{v}_0 + \gamma_0 \mathbf{v}_1) + \rho_0 (\gamma_1 \mathbf{v}_0 + \gamma_0 \mathbf{v}_1) \cdot \nabla (\gamma_0 \mathbf{v}_0) \\ \quad + \rho_1 \gamma_0 \mathbf{v}_0 \cdot \nabla (\gamma_0 \mathbf{v}_0) = (\nabla \times \mathbf{B}_0) \times \mathbf{B}_1 + (\nabla \times \mathbf{B}_1) \times \mathbf{B}_0 + \mathbf{B}_0 \times \frac{\partial \mathbf{E}_1}{\partial t} + \mathbf{E}_1 (\nabla \cdot \mathbf{E}_0) + \mathbf{E}_0 (\nabla \cdot \mathbf{E}_1), \\ \dots \text{ [lots of algebra] } \dots \end{array} \right.$$

- Expressing $Q_1 \propto \exp(i\omega t - im\phi - ikz)$ and ≈ 12 pages of math later:

$$\left\{ \begin{array}{l} D \frac{d\xi_{1r}}{dr} = \left(C_1 + \frac{C_2 - Dk'_B}{k_B} - \frac{D}{r} \right) \xi_{1r} - C_3 \Pi_1 \\ D \frac{d\Pi_1}{dr} = \left[A_1 D - \frac{\rho_0 \gamma_0^2 v_{0\phi}^2}{r} \left(C_1 + \frac{C_2 - Dk'_B}{k_B} + \frac{C_4}{r} + C_5 \right) \right] \xi_{1r} + \left[\frac{1}{r} \left(\rho_0 \gamma_0^2 v_{0\phi}^2 C_3 - 2D + \frac{C_6}{r} + C_7 \right) \right] \Pi_1 \end{array} \right.$$

ODE: Boundary Value Problem

- System of 2 ODEs in complex variables ξ_{1r} (displ.) and $\Pi_1 = B_0 \cdot B_1 - E_0 \cdot E_1$:

$$\begin{cases} D \frac{d\xi_{1r}}{dr} = \left(C_1 + \frac{C_2 - Dk'_B}{k_B} - \frac{D}{r} \right) \xi_{1r} - C_3 \Pi_1 \\ D \frac{d\Pi_1}{dr} = \left[A_1 D - \frac{\rho_0 \gamma_0^2 v_{0\varphi}^2}{r} \left(C_1 + \frac{C_2 - Dk'_B}{k_B} + \frac{C_4}{r} + C_5 \right) \right] \xi_{1r} + \left[\frac{1}{r} \left(\rho_0 \gamma_0^2 v_{0\varphi}^2 C_3 - 2D + \frac{C_6}{r} + C_7 \right) \right] \Pi_1 \end{cases}$$

- We solve the system for $0 < r < \infty$ with boundary conditions:
 - $r = 0$: series expansion (ODE singular at $r = 0$)
 - $r \rightarrow \infty$: Asymptotic solutions have to decay and no incoming wave is allowed (Sommerfeld condition).
- For finding the eigenvalue ω we use a shooting method with a complex secant root finder: forward and backward solutions are matched at an intermediate radius¹.

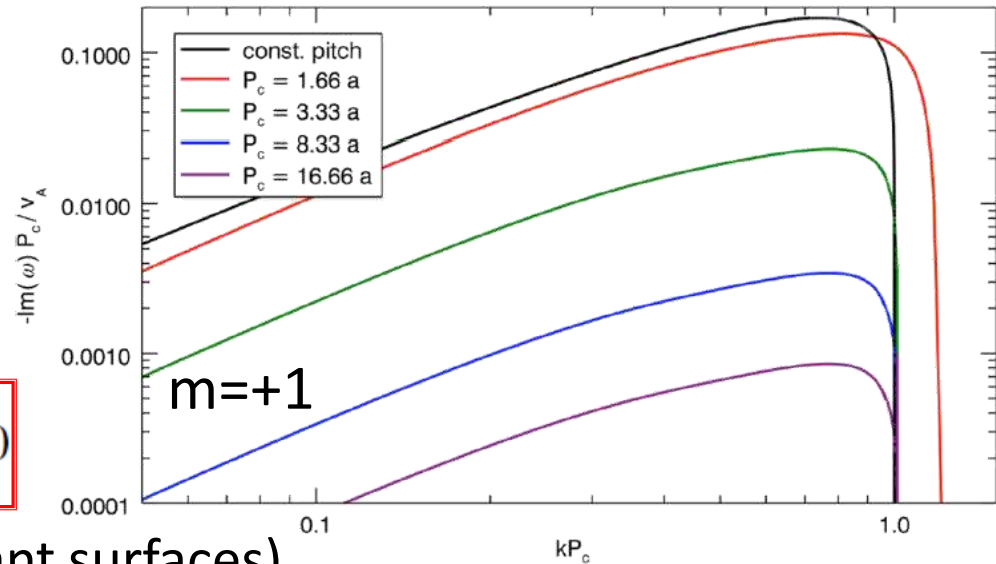
¹Bodo et al, MNRAS (2013) 434, 303

Results: static case ($\gamma_c = 1$)

- Only CD mode present.
- **Resonant condition** critical for determining instability:

$$k \cdot B = kB_z + \frac{m}{r} B_\phi = kP + m = 0$$

(no magnetic tension on resonant surfaces)

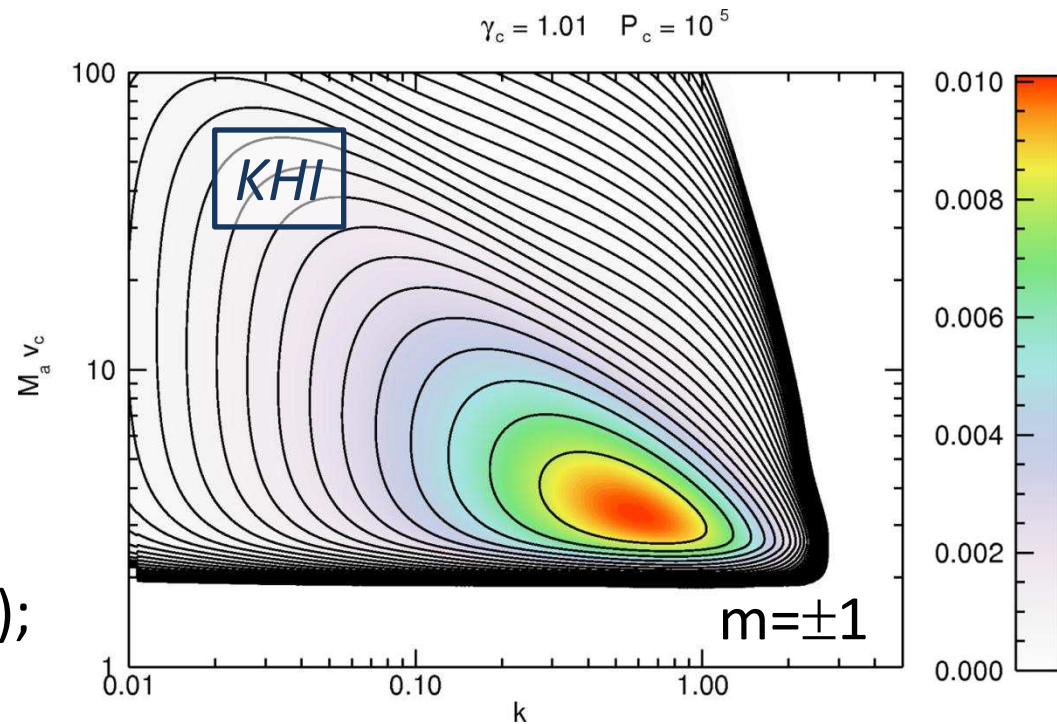


- since $P=P(r) < 0$ this is verified only for $m = +1 \rightarrow$ **“Kink” mode**
- Instability present for all wavenumbers $k < 1/P_c$;
- In the limit $P_c/a \gg 1$, we verify the asymptotic scaling

$$\text{Im}(\omega) \sim \frac{v_A}{P_c} \left(\frac{a}{P_c} \right)^2 f(k P_c)$$

$$\gamma_c = 1.01, P_c = 10^5$$

- For large Pitch, $B \approx B_z$ (longitudinal field)
- only KH mode is present for $m = \pm 1$ (coincident)
- CD mode is absent (stable);
- Jet stability limit for $M_a v_c \sim 2$ which gives the limit $v_c < 2 v_a$

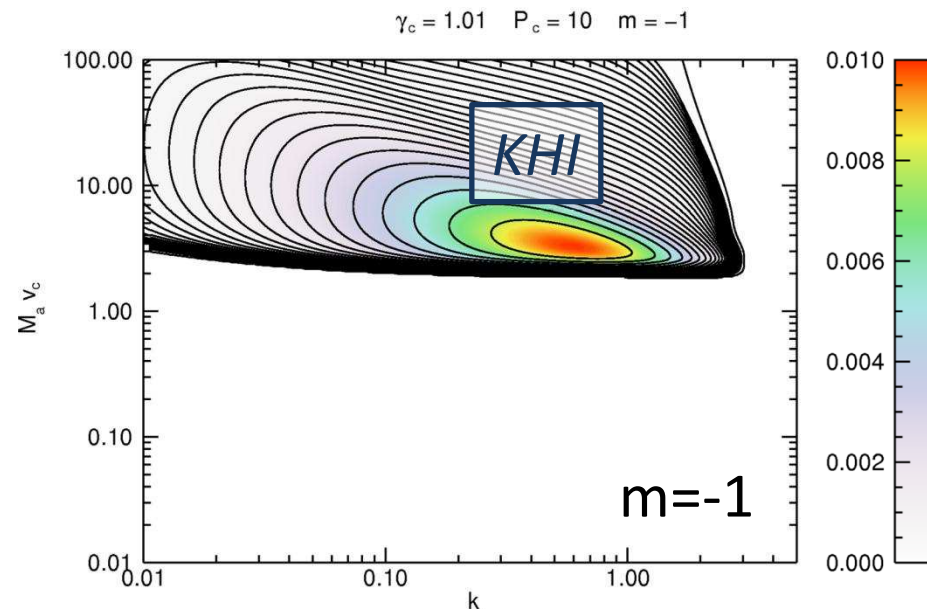
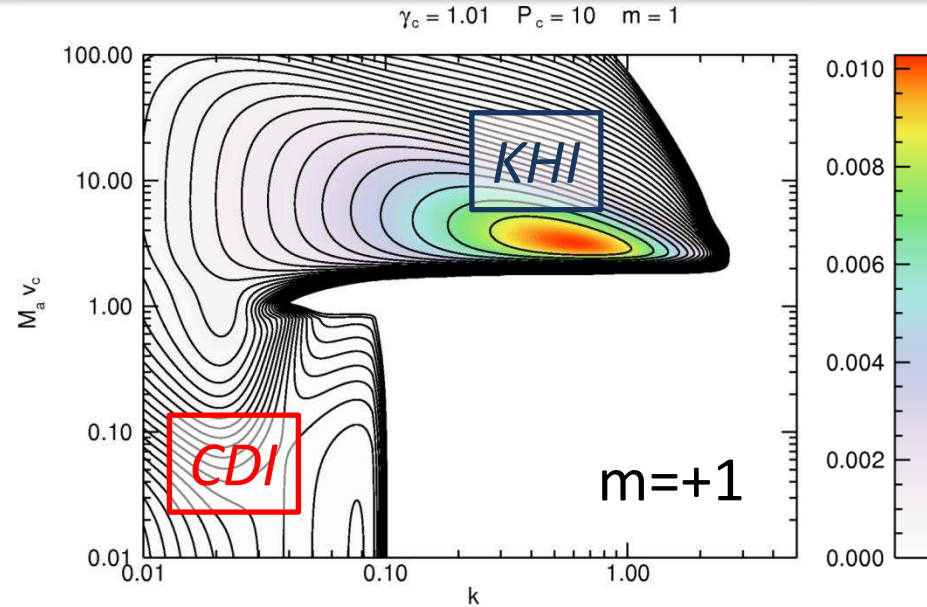


- Remind that

$$M_a v_c = \frac{\gamma_c v_c}{|\mathbf{B}| / \sqrt{\rho}}$$

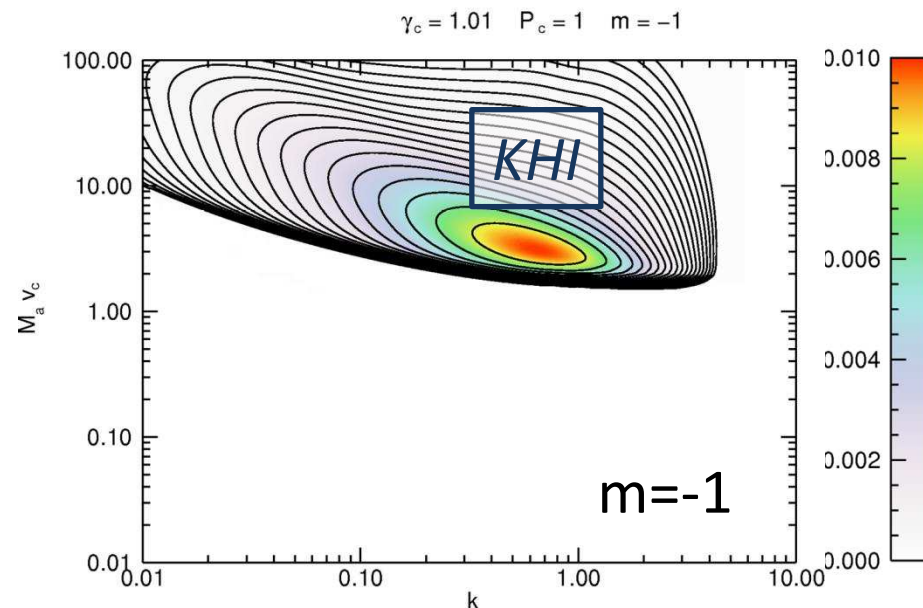
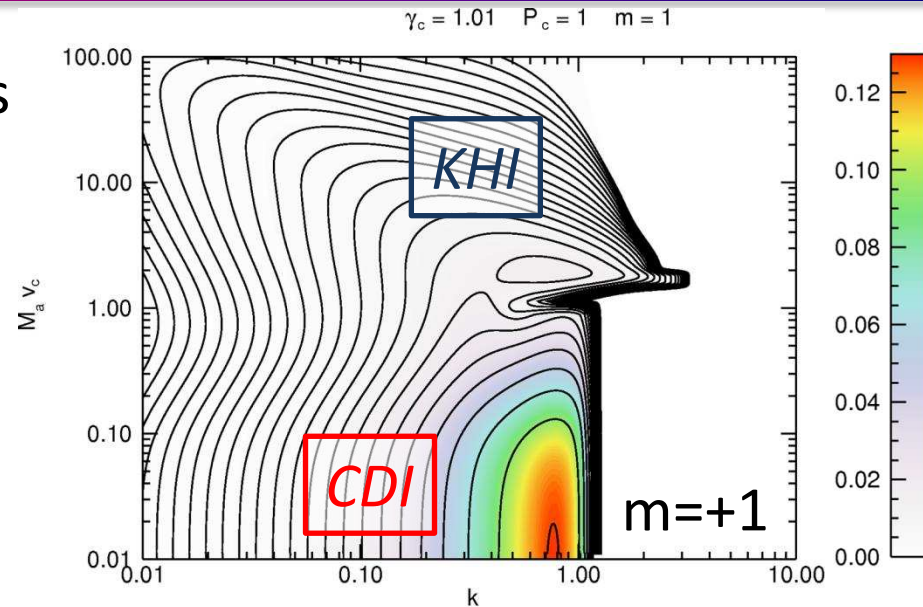
$$\gamma_c = 1.01, P_c = 10$$

- Both KHI and CDI are present;
- KHI present for $m = \pm 1$:
Increasing $M_a v_c$ shifts the maximum to smaller k , $\omega_{\max} \sim 1/M_a v_c$
- CDI absent for $m = -1$
(resonant condition cannot be satisfied)
- $\omega_{CD} \ll \omega_{KH}$
- CDI stability limit for $kP_c = 1$
stable $\rightarrow k > 0.1$



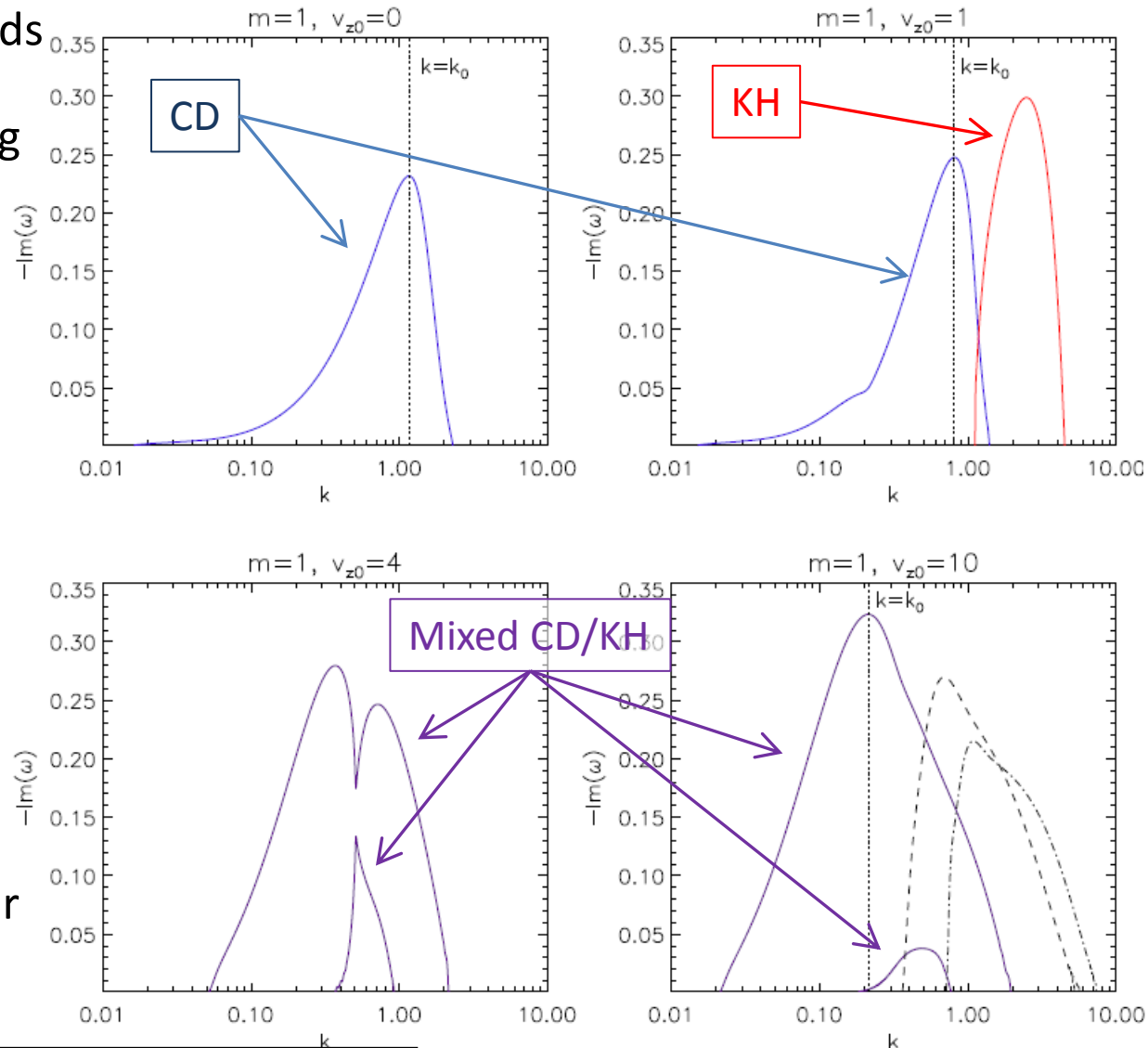
$$\gamma_c = 1.01, P_c = 1$$

- The CDI ($m=+1$) moves towards higher k ;
- ω_{CD} scales as $\sim 1/P_c^3$;
(as in the static case)
- $\omega_{CD} \gg \omega_{KH}$
- KHI presents only slight differences with the cases at larger P_c .



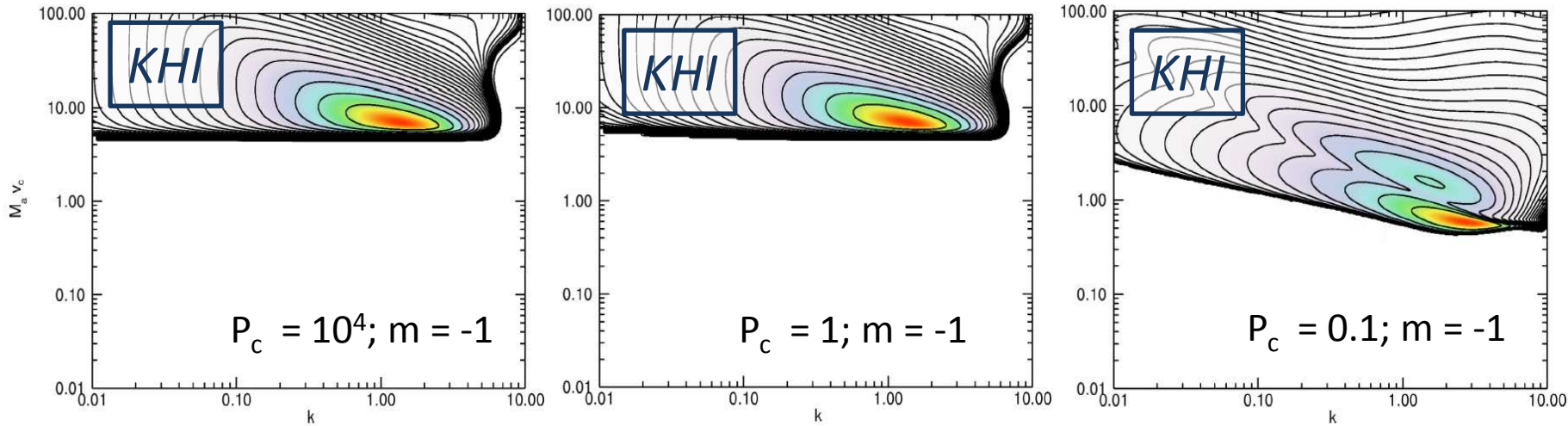
Mode Transition

- Increasing jet velocity leads to mode overlapping, merging and then splitting in more branches¹.
- At $v_z=4$ we have a mode with larger ω and a 2nd smaller mode.
- Both have mixed CD/KH properties.
- KHI and CDI are expected to play a role although it may not be possible to unequivocally isolate their contributions.

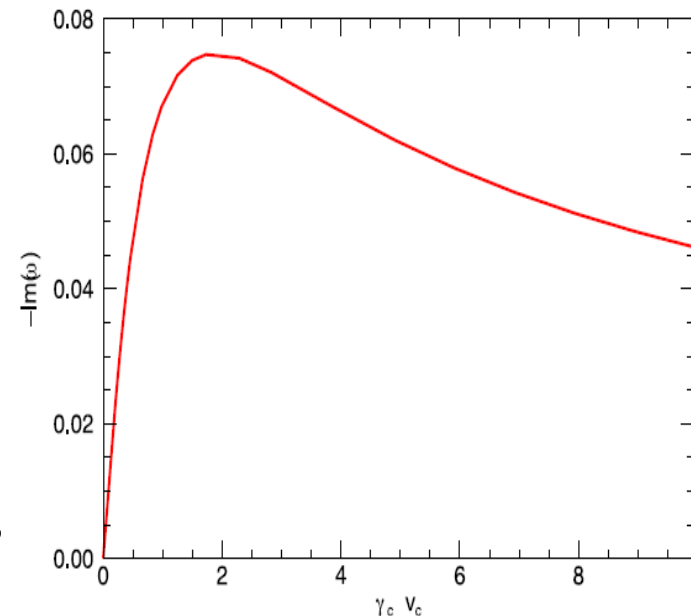


¹Anjiri et al, MNRAS(2014) 442, 2228

Relativistic Flow ($\gamma_c = 10$): KH mode

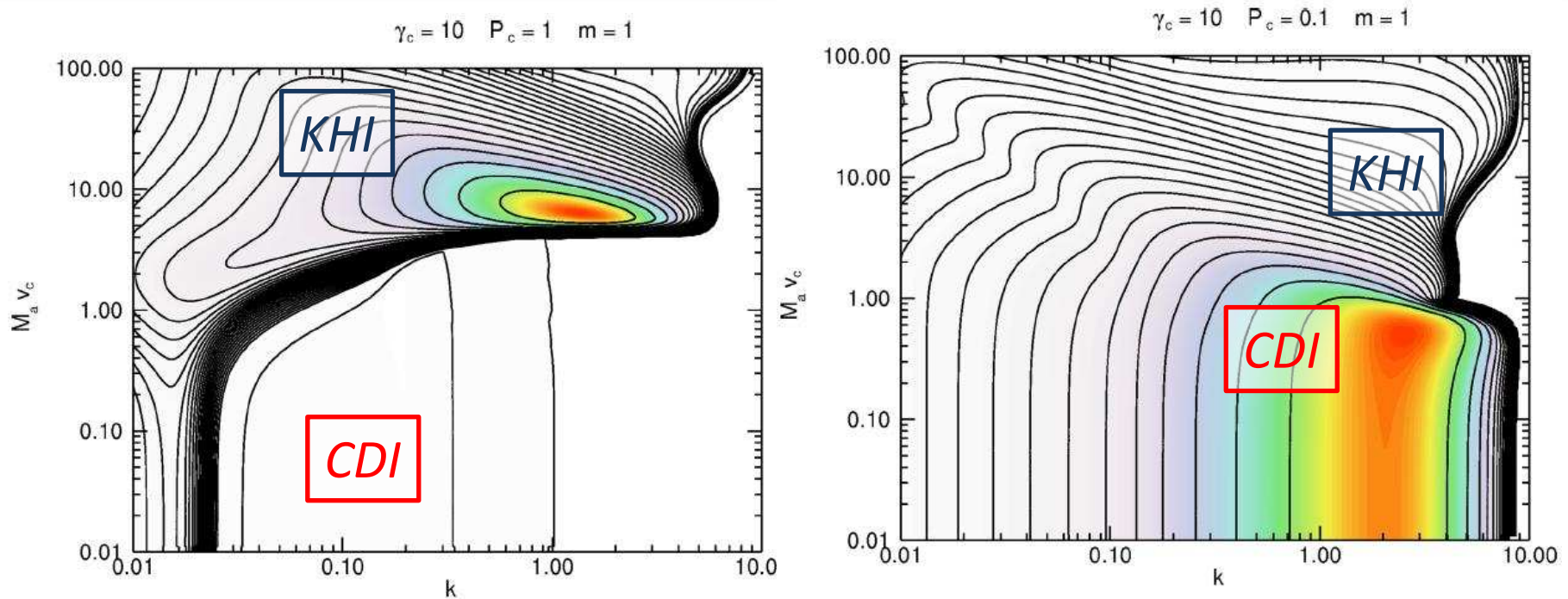


- Stability boundary of KHI and ω_{\max} move at larger values of $M_a v_c$ with respect to classical cases¹;
- For $P_c < 1$, KHI boundary moves towards smaller values of $M_a v_c \sim 2$ (stabilizing longitudinal component weakens)
- For increasing γ_c the maximum ω decreases



¹Osmanov et al, A&A (2008) 490, 493

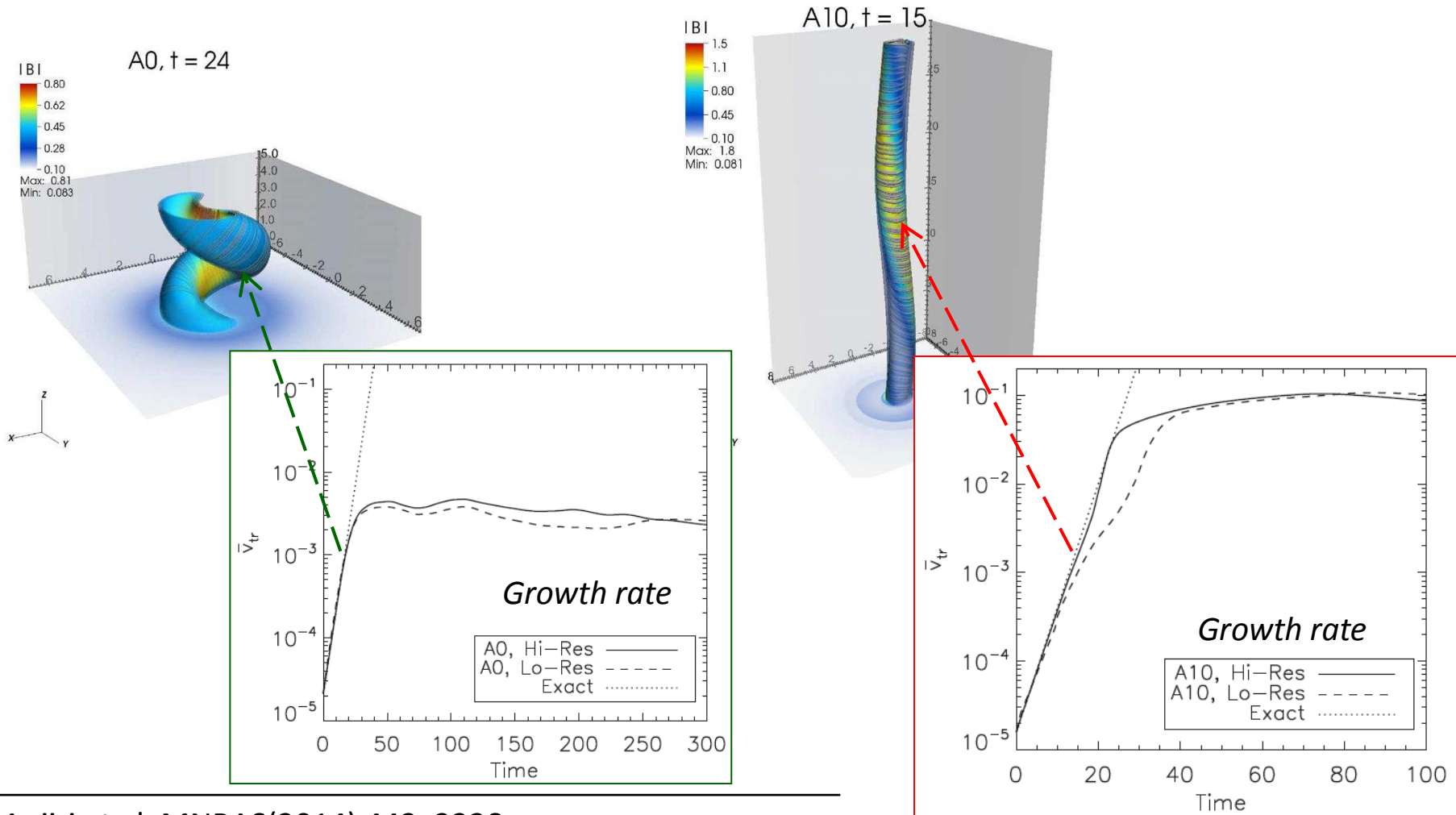
Relativistic Flow ($\gamma_c = 10$): CD mode



- CD: mode splits in two branches: an inner mode concentrated inside the jet and an outer mode outside the jet: condition $kP(r) = 1$ cannot be fulfilled inside the shear (pitch steeper)
- The relative importance of the two branches depends both on the current concentration (a) and Lorentz factor γ_c .
- CD: scaling of the inner mode $\omega_{CD} \sim 1/(P_c^3 \gamma_c^4)$

Numerical Simulations: linear phase

- Numerical simulations confirm analytical predictions¹: linear growth correctly reproduced but high resolution required (> 20 pt / jet radius)

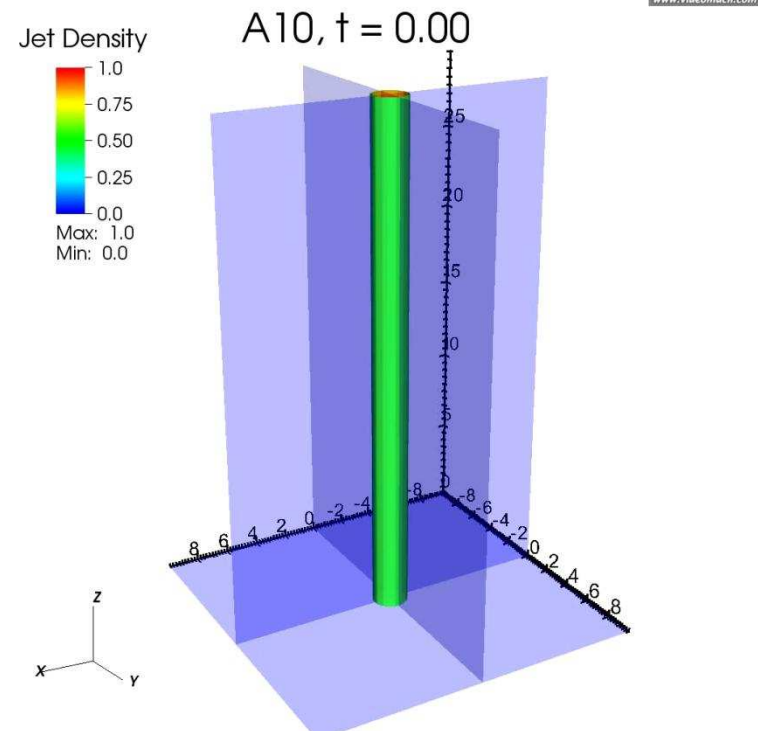
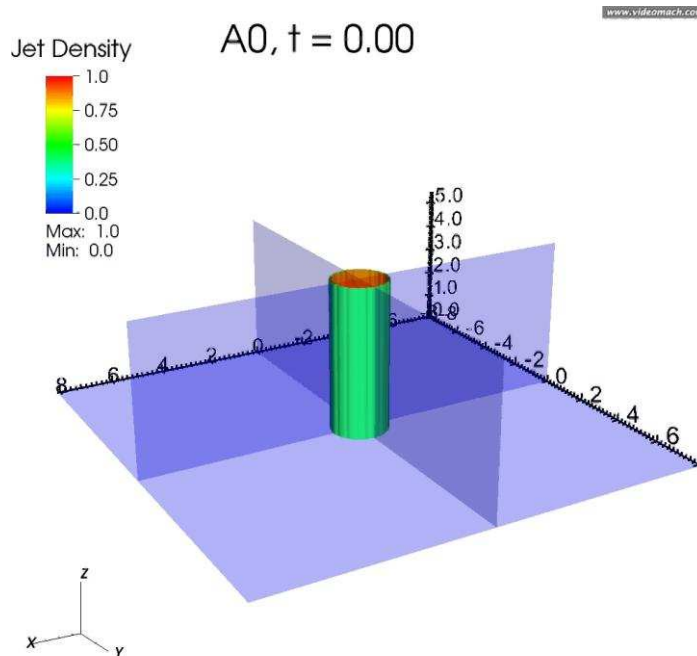


¹Anjiri et al, MNRAS(2014) 442, 2228

Transition to nonlinear phase

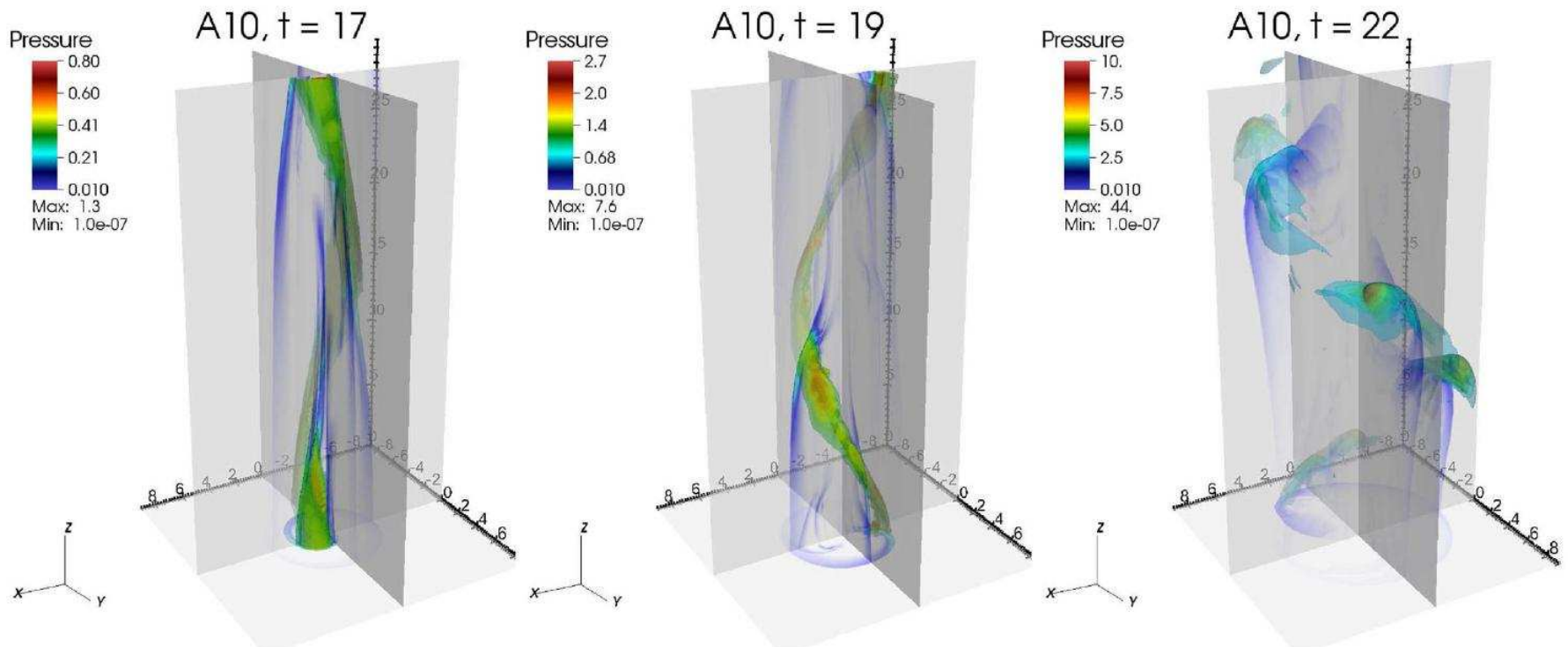
- *Static jet*: the initial displacement grows into a twisted helical deformation;

- **Super-Alfvénic jet** ($v/v_A=10$): linear growth accompanied by oblique perturbations steepening into shocks;
- *Large wavelength non-axisymmetric deformation* as well as small-scale surface modes;



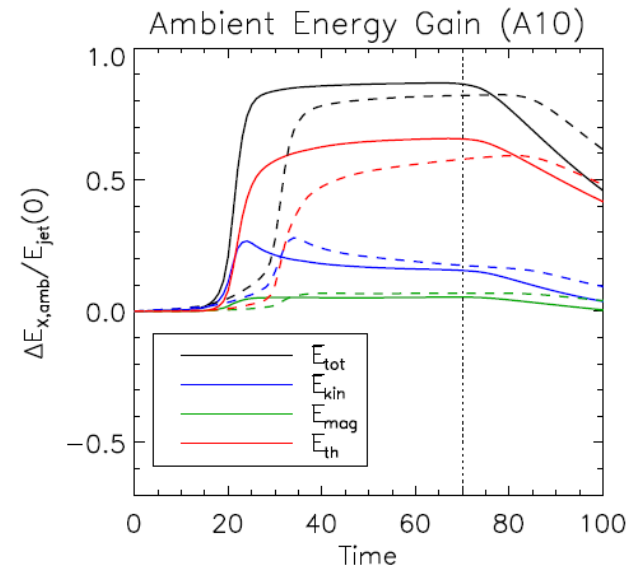
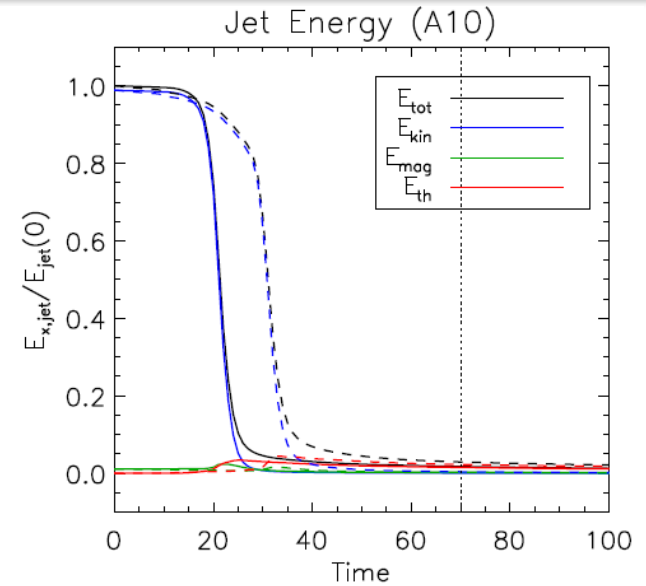
Nonlinear evolution

- Fast jet disrupted: presence of KHI gives rise to small-scale disturbance that crumble and grow on top of helical deformations.
- Instability spreads and redistribute the initial jet material and momentum over a larger surface area with consequent reduction of the jet average velocity and hence favouring jet braking in few Alfvén time-scales .



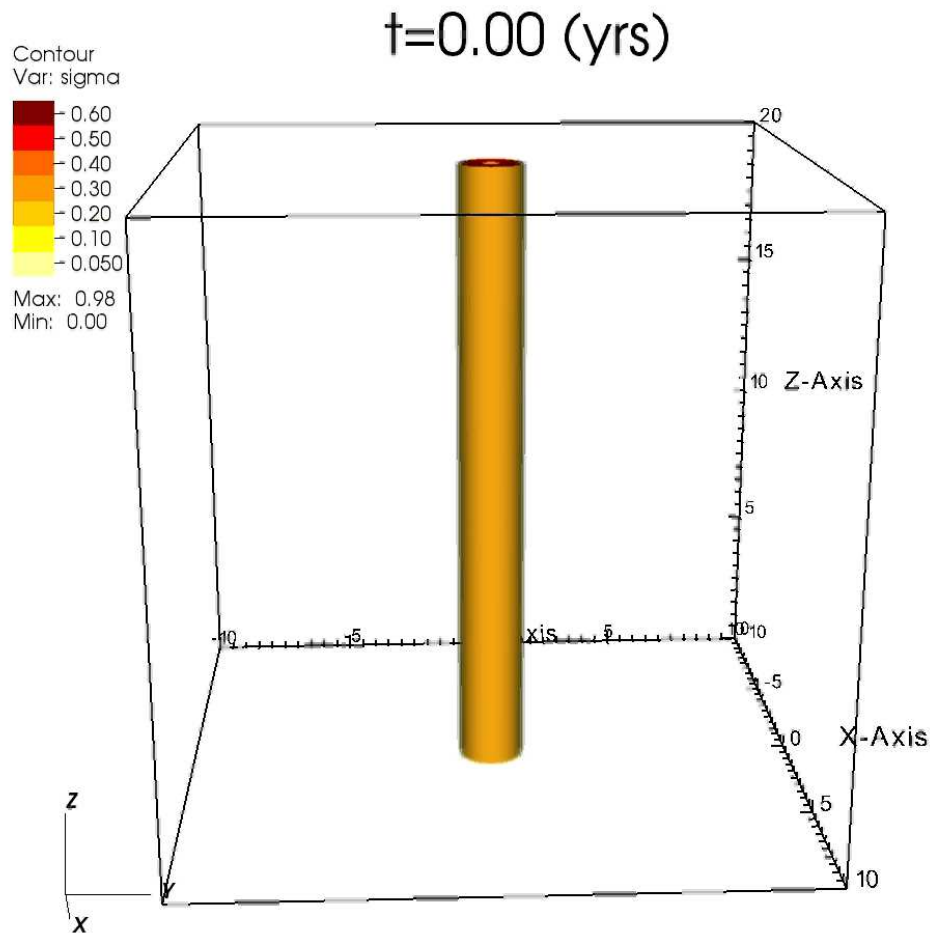
Energy Budget

- Shocks provide efficient dissipation mechanism of mechanical energy;
- Jet becomes forcefully disrupted on a rapid time scale;
- Jet loses up to $\approx 80\text{--}90\%$ of its initial energy which becomes available to the ambient medium mostly in the form of heat and, secondly, kinetic energy.



Pressure-Balanced Jets (not force-free)

www.videomach.com



- Purely toroidal field, pressure-balanced jet:

$$\frac{dp}{dr} = J_z B_\phi, \quad \mathbf{J} \perp \mathbf{B}$$

- No helical displacement
- Deflection caused by growth of $m=\pm 1$ KH and PD modes.
- No CDI !!

Summary

- Instabilities in jets responsible for morphology, mom. and energy dissipation;
- Analytical study essential for the interpretation of numerical results: non-rotating, force-free, cold jets may be prone to **KHI** and **CDI**:
 - **KHI** prevails in **matter-dominated** flows: k_{\max} and $\omega(k_{\max}) \sim 1/M_a v_c$. Weak dependence on the pitch. Stabilization at large γ , merging at small Pitch.
 - **CDI** prevails in **magnetically-dominated** flows: $k_{\max} \sim 1/P_c$ and $\omega(k_{\max}) \sim 1/P_c^3$. High γ steepen the pitch profile inducing mode stabilization in regions where the return current is found \rightarrow mode splitting. Mergin with KH in super-Alfvenic flows.
- Results confirmed by 3D numerical simulations.
- Nonlinear evolution of CDI feature large helical displacements...
- Combined action of KHI and CDI \rightarrow efficient mechanism to transfer momentum and energy to ambient during nonlinear stages.

THE END

*Thank you
for
your attention*